JOURNAL OF GEOPHYSICAL RESEARCH, VOL. 104, NO. E6, PAGES 14,149–14,157, JUNE 25, 1999

Radio atmospheric propagation on Mars and potential remote sensing applications

Steven A. Cummer and William M. Farrell
Laboratory for Extraterrestrial Physics, NASA Goddard Space Flight Center, Greenbelt, Maryland

Abstract. We theoretically analyze the propagation of very low frequency (VLF) and extremely low frequency (ELF) electromagnetic energy in the spherical waveguide formed by the ground and ionosphere of Mars to investigate the possibility of using such signals to remotely sense Martian ground conductivity and ionospheric parameters. This energy is presumed to be radiated from an electrical discharge in a Martian dust storm. Using a synthesis of observed and modeled Martian ionospheric and ground parameters and assuming a discharge current similar to that in a terrestrial lightning discharge, we calculate radio atmospheric spectra and waveforms for a variety of discharge orientations and observed electromagnetic field components. A number of characteristics of the modeled Martian radio atmospherics (sferics) are found to be significantly different from those of terrestrial sferics, and we discuss how these features could provide information regarding the Martian ionosphere. We also show that measurements of VLF and ELF attenuation rates could provide a measurement of large-scale ground conductivity to a depth of a few kilometers or more, thereby providing a technique for probing large-scale subsurface geological features which affect bulk conductivity, such as areas containing ice or water.

1. Introduction

The existence of electrical discharges generated by dust storms on Mars is an intriguing possibility from both a scientific and practical standpoint. Terrestrial dust devils are known to be electrically active [*Crozier*, 1964], and volcanic eruptions can be accompanied by spectacular electrical discharges [*Anderson et al.*, 1965]. Experimental [*Eden and Vonnegut*, 1973] and theoretical [*Farrell et al.*, 1999] investigations of dust grain electrification have found that both glow and filamentary discharges on Mars could be generated in swirling dust storms. Should such discharges be found to exist, the very low frequency (VLF, 3–30 kHz) and extremely low frequency (ELF, 3–3000 Hz) electromagnetic radiation from them could be used as on Earth for probing the ionosphere [*Cummer et al.*, 1998] and subsurface ground [*Goldman and Neubauer*, 1994].

In this work, we presuppose the existence of electrical discharges on Mars that, like terrestrial thunderstorm lightning, radiate electromagnetic energy in the VLF and ELF bands. Such discharges would be similar to the filamentary discharges observed in the lab by *Eden and Vonnegut* [1973] and are distinct from the glow (or Paschen) discharge which radiates at much higher frequencies. *Farrell et al.* [1999] explored the possibility of dust devil electrification and found that filamentary discharges from Martian dust storms could be produced by the expected level of charge separation, while this paper focuses primarily on the radiation and propagation of the VLF and ELF electromagnetic energy created by such discharges. Because of the transient nature of the source (i.e., discharge current), the radiated energy is contained in short-timescale signals which are commonly termed radio atmospherics or sferics. We investigate the propagation of these sferics in the spherical waveguide formed by the Martian ground and ionosphere using a numerical propagation model. We calculate radiated VLF and ELF magnetic and electric field spectra and waveforms for a variety of source current orientations and for waveguide characteristics (i.e., the ionosphere and ground) appropriate for Mars. Not surprisingly, we find that Martian sferics have some significant differences from their terrestrial counterparts which are primarily due to the assumed lossier Martian ionosphere and less conducting Martian ground.

Not only would the presence of VLF and ELF signals like those presented here be likely confirmation of electrical discharges on Mars, but because their propagation is controlled largely by the lower ionosphere and ground, Martian sferics would provide a technique for remotely sensing these two media. In particular, we demonstrate how VLF and ELF attenuation rates measured from sferics could be used to probe the large-scale Mar-

Paper number 1998JE000622.
0148-0227/99/1998JE000622$09.00

tian ground conductivity. A conductivity significantly higher than that of the surface dust layer could indicate the presence of high-conductivity minerals or even subsurface ice or water. These remote sensing techniques only require a localized source of VLF and ELF waves, and waves radiated by any such source could possibly be used in a similar manner.

Although we arbitrary assume discharge currents similar to those on Earth, the results of this work can be adapted to other source timescales and amplitudes. The propagation problem is linear, so sferic spectra and waveforms from more slowly varying sources can be constructed by a superposition of the waveforms presented herein.

Related work has been reported by *Sukhorukov* [1991], who calculated the Martian Schumann resonance frequencies and attenuation rates using an analytical approximation of the Martian ionosphere. Schumann resonances play a strong role in the global-scale propagation of electromagnetic waves of frequency less than 50 Hz [*Sentman*, 1989], while this work focuses on higher-frequency propagation over shorter distances.

2. VLF Propagation Modeling

We use the sferic propagation model described by *Cummer et al.* [1998], which is based on a single-frequency VLF and ELF propagation model [*Pappert and Ferguson*, 1986]. The latter model solves the time-harmonic (i.e., single frequency) propagation problem using mode theory [*Budden*, 1961], in which the fields at a distance from the source are described as a sum of independently propagating waveguide modes. In the locally Cartesian coordinate system used in this work, x is horizontal in the direction of propagation, z is vertical and perpendicular to the ground, and y is horizontal and transverse to the direction of propagation. As an example of this model, the transverse horizontal magnetic field B_y at a distance x along the ground from a vertical electric dipole source transmitting at an angular frequency of ω is [*Pappert and Ferguson*, 1986]

$$B_y(\omega,x) = -\mu_0 k^{\frac{1}{2}} M_e(\omega) \left[R \sin\left(\frac{x}{R}\right)\right]^{-\frac{1}{2}} \cdot \left(\frac{\pi}{2}\right)^{-\frac{1}{2}} e^{\frac{i\pi}{4}} \sum_n \Lambda_{tn}\,\Lambda_{rn}\, e^{-ikx\sin\theta_n}. \quad (1)$$

The wavenumber k is given by $k = \omega/c$, $M_e(\omega)$ is the vertical electric dipole moment of the source (and is related to the source current by $M_e(\omega) = lI(\omega)/i\omega$, where I is the source current amplitude and l is the length of the current channel), and the term $\left[R\sin\left(\frac{x}{R}\right)\right]^{-\frac{1}{2}}$ accounts for the spreading of the fields over a spherical surface of radius R (note that this term is equivalent to $x^{-\frac{1}{2}}$ over short distances). The summation includes the significant waveguide modes (strongly attenuated modes are excluded as they contribute negligibly to the total field), each of which has an index of refraction given by the sine of the corresponding eigenangle θ_n. The excitation and receiver factors Λ_{tn} and Λ_{rn} contain the altitude dependence of the fields and also depend on the observed field component. The reader is referred to *Pappert and Ferguson* [1986] and references therein for further details concerning this model.

To calculate the fields from a broadband source, one simply needs to calculate $B_y(\omega)$ (or any other field component) over the range of frequencies significant to the problem at hand. The resulting sferic spectrum can be converted to a time domain waveform with an inverse Fourier transform operation, which can be approximated by the inverse fast Fourier transform [*Oppenheim and Schafer*, 1989, p. 514].

This ELF-VLF propagation model allows for an arbitrary homogenous ground conductivity and permittivity as well as arbitrary inhomogeneous altitude profiles of ionospheric electron density and electron-neutral collision frequency. While there are approximate analytical models that describe ELF propagation under an exponentially varying ionospheric conductivity [*Greifinger and Greifinger*, 1986, and references therein], they are not directly applicable to this work because they generally assume a perfectly conducting ground. As discussed above, the Martian ground is more likely a poor conductor at ELF and VLF. The source lightning current parameters of our propagation model (current waveform, orientation, and altitude) can also be chosen freely. The details of these model parameters are discussed in section 2.1.

2.1. Waveguide Parameters

Long-distance ELF-VLF propagation is controlled by the ground and ionosphere which form the upper and lower boundaries of the waveguide. We assume initially that the Martian ground is homogeneous with conductivity $\sigma_g = 10^{-7}$ mho m^{-1}, a relative permittivity $\epsilon_{rg} = 5$, and a relative permeability of unity. This permittivity is consistent with Martian surface parameters measured by VHF scattering [*Tyler et al.*, 1976]. In constrast, it is difficult to choose an appropriate σ_g because the Martian ground conductivity is not well quantified. *Olhoeft and Strangway* [1974] estimated a Martian surface conductivity of $\sigma < 10^{-12}$ from an analysis of lunar soil samples. However, at these low values, the ground is very poorly conducting at VLF and ELF, and thus the skin depth (the depth at which a propagating wave will have attenuated to e^{-1} of its initial value) is extremely long. Under these conditions, ELF-VLF propagation is influenced by the ground conductivity to a depth of possibly tens of kilometers, and a surface layer of low conductivity will not strongly affect the propagation. For this reason, we assume a homogeneous ground conductivity (10^{-7} mho m^{-1}) between that of the surface dust and that typical of terrestrial ground [*Goldman and Neubauer*, 1994]. Our assumption that the ground has the permeability of free space may not be valid because of the high concentration of iron in Martian soil. However, the theoretical relative

permeability reported by *Olhoeft* [1998] of ~1.5 is small enough to have only a very small effect on the results reported here. In section 4 we consider the possibility that the homogeneous Martian ground parameters are significantly different than these assumed values.

On a more global scale, our propagation model does account for the spherical geometry of the waveguide. However, the model does not include fields that propagate in a direction other than the shortest great circle path between source and receiver. Because of the relatively high attenuation rates at the frequencies considered herein, these around-the-world signals are not important except for locations near the antipode of the source, where our model is not valid. We also assume that the Martian surface is uniform in altitude, as we are studying ELF-VLF propagation on Mars in a general sense. This is clearly not the case on some paths, as Olympus Mons protrudes 30 km above the mean Martian surface, and surface variations of this magnitude would affect ELF-VLF propagation.

For the purposes of low-power ELF-VLF wave propagation, the Martian ionosphere can be fully characterized by its free electron density, electron-neutral collision frequency, and ambient magnetic field (which we take to be zero) [*Budden*, 1985, p. 4]. The momentum-transfer electron-neutral collision frequency altitude profile we use in this work is plotted in Figure 1. The profile was calculated using the theory of *Banks and Kockarts* [1973, p. 188] from atmospheric pressure and temperature from a model Martian atmosphere [*MacElroy et al.*, 1977] and the electron-CO_2 collision cross section from *Hake and Phelps* [1967]. Electron-ion collisions are negligible compared to the electron-neutral collision frequency for the altitudes less than 200 km considered here. Plotted for comparison is a representative electron-neutral collision frequency profile for Earth which is a concatenation of the profile used by *Cummer et al.* [1998] and that from *Budden* [1985, p. 12]. Although the atmospheric pressure on Mars is roughly a factor of 100 smaller than on Earth, the substantially

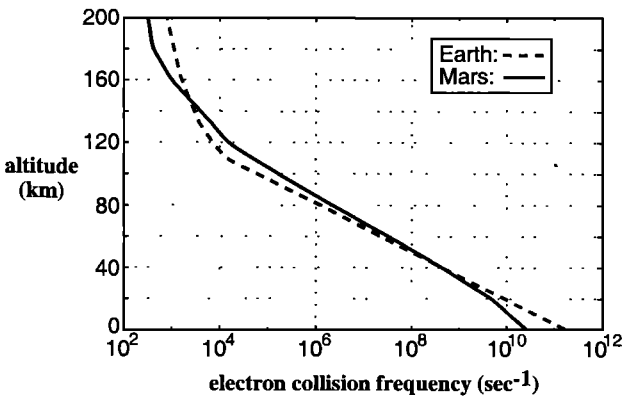

Figure 1. Martian and terrestrial momentum-transfer electron-neutral collision frequency profiles.

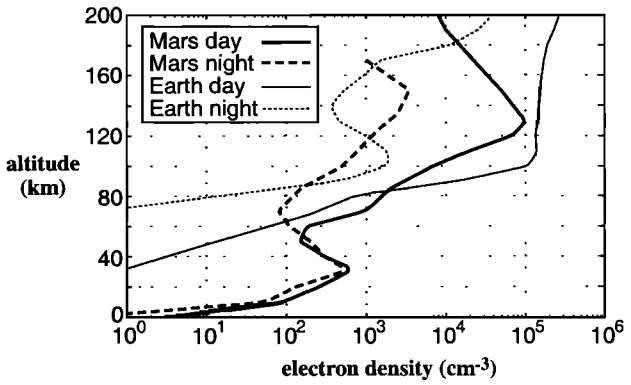

Figure 2. Martian and terrestrial electron density profiles for day and night.

larger collision cross section for CO_2 compensates for this and leads to a profile close to that on Earth.

The Martian electron density altitude profile has been measured with both in situ [*Hanson et al.*, 1977] and radio occultation [*Zhang et al.*, 1990] techniques, but nearly all of these measurements have been made at altitudes greater than 110 km. From a combination of observation and theory, we have assembled representative nighttime and daytime Martian electron density profiles which are plotted in Figure 2. The lower portions (<80 km) of both profiles are theoretical profiles from *Whitten et al.* [1971], while the upper portions (>110 km) are experimental profiles from *Zhang et al.* [1990] and *Hanson et al.* [1977] for nighttime and daytime, respectively. Plotted for comparison are representative terrestrial electron density profiles for midnight and noon obtained from the 1995 International Reference Ionosphere [*Bilitza*, 1997]. Our assumption of a lack of a significant magnetic field on Mars means that ions do not contribute significantly to the ionospheric index of refraction for any wave frequency [*Budden*, 1985, p. 55]. Thus we neglect the effects of ionospheric ions on the wave propagation.

The primary difference between the terrestrial and Martian electron density profiles is the presence of a distinct ionization layer near 30 km on Mars which is produced by incoming cosmic rays. However, this cosmic ray layer is not a significant reflector for VLF frequencies. Because the collision frequency is high at this altitude, the high N_e has only a very small effect on the index of refraction n and therefore does not significantly affect the VLF propagation. For $f \lesssim 300$ Hz, however, n deviates from unity significantly near or in this layer, and its presence does influence ELF propagation.

2.2. Source Parameters

We assume throughout this work that the current flowing in a Martian lightning channel varies as

$$I(t) = I_0 \left[\exp(-bt) - \exp(-at)\right] \text{ Am}, \qquad (2)$$

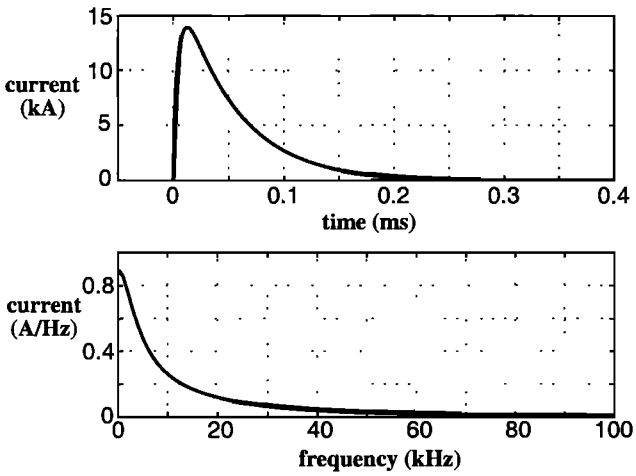

Figure 3. Lightning current waveform and spectrum used as a radio atmospheric source throughout this work.

and that the lightning channel extends either horizontally or vertically for a distance of 1 km. Because the source is embedded in a waveguide, a source in any orientation will radiate fields that are observable in any azimuthal direction, even in a direction of null of the individual radiating dipole. Throughout this work, we use values typical for a vertical terrestrial discharge of $I_0 = 20$ kA, $a = 2\times10^5$ s^{-1}, and $b = 2\times10^4$ s^{-1} [*Jones*, 1970]. These discharge parameters produce a peak current of ~14 kA and a total charge displacement of 0.9 C along the 1 km channel. Figure 3 shows this current waveform and its spectrum. On the basis of the estimates of *Farrell et al.* [1999], this charge transfer is consistent with the charging which could be supported by a large Martian dust devil of 5 km radius and 10 km altitude.

Of course, Martian discharge characteristics may be significantly different from those assumed in terms of amplitude or timescale. However, since the propagation problem is linear, the results presented here can be scaled appropriately to find sferic amplitudes for any source amplitude. Sferic waveforms radiated by slower sources can be estimated by a superposition (i.e., convolution) of the waveforms presented herein. Sferic waveforms radiated by faster sources will not be drastically different than those presented here because the assumed discharge timescale is relatively fast compared to the main radiated frequency components considered here.

3. Sferic Waveforms and Spectra on Mars

Our ELF-VLF propagation model allows for an arbitrary specification of the discharge orientation (i.e., vertical or horizontal) and of the observed electromagnetic field component, and below we present sferic waveforms and spectra from a number of different source orientations and field components. To calculate the sferic waveforms from the spectra produced by the frequency domain model, we must assume that there is an upper limit to the frequency range which contributes significantly to the waveform; that is, we must terminate the integration at some finite frequency. In a practical sferic receiving system, this upper limit would be imposed by a low-pass filter with a cutoff frequency dictated by the rate at which the waveform was sampled. In this work, we include the effect of a fourth-order low-pass filter with a cutoff frequency of 25 kHz, which essentially limits the maximum sferic bandwidth to ~40 kHz. Similarly, there is a lower limit to the frequency response of most receivers, and we have also included the effect of a single-pole high pass filter with a -3 dB cutoff frequency of 100 Hz.

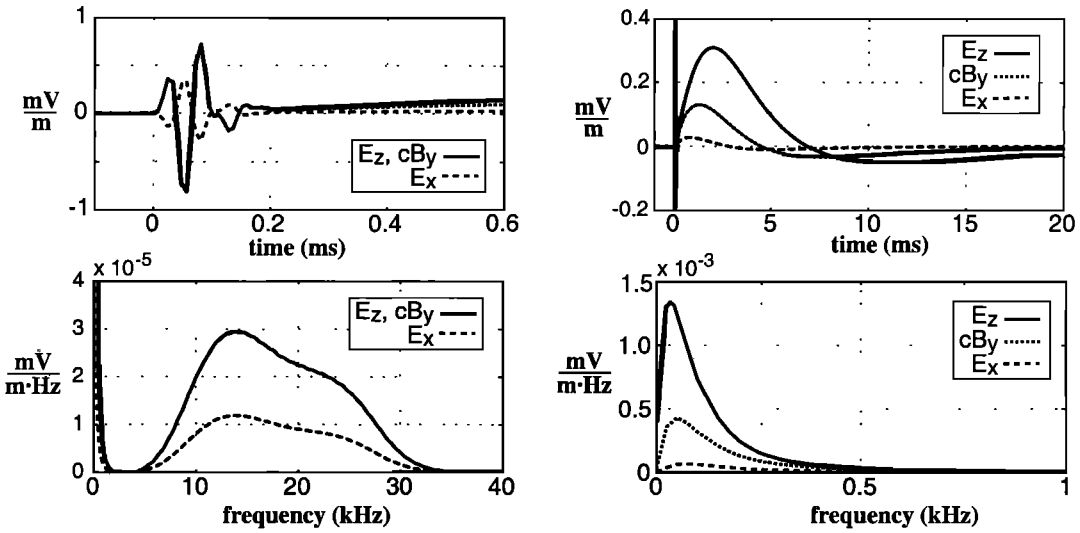

Figure 4. E_z, cB_y, and E_x sferic waveforms and spectra observed at a propagation distance of 1000 km under a daytime Martian ionosphere. The source current is vertically oriented at ground altitude.

Throughout this work, we only consider sferics calculated using the daytime Martian ionosphere shown in Figure 2. Model calculations show that the expected difference between nighttime and daytime propagation is small. All fields presented in this work are assumed to be observed at ground altitude. Some of the waveforms in the plots below have been inverted to allow an easier comparison of the different fields.

3.1. Sferics From a Vertical Discharge

Figure 4 shows E_z, E_x, and cB_y waveforms and spectra observed 1000 km from a vertical source discharge. The source is at an altitude of 0 km (at the ground), and the source current varies as (2). They are each shown on two different scales to highlight the ELF and VLF regimes, which are almost completely distinct because of the large signal attenuation from 2–5 kHz. We multiply B_y by the speed of light in a vacuum c to convert it to units of electric field to allow a direct comparison of the field component magnitudes. In the case of a vertical source, cB_y is nearly identical to E_z for VLF frequencies observed on the ground.

Because the waveguide considered here is isotropic (a consequence of the absence of any ambient magnetic field), a vertically oriented source will only excite the transverse magnetic (TM) fields, namely, E_z, B_y, and E_x [*Ramo et al.*, 1984, p. 404], so for this source orientation the other field components are zero. There are fundamental differences in the field components present in terrestrial and Martian sferics which are discussed in detail in section 3.3.

3.2. Horizontal Discharge

A horizontal current source oriented parallel to the propagation direction (the "end-fire" configuration) excites the same TM fields excited by a vertical dipole [*Pappert and Ferguson*, 1986], and for this reason, the fields radiated from such a current source are very similar to those radiated from a vertical dipole. Figure 5 shows E_z, E_x, and cB_y waveforms and spectra for an end-fire horizontal source at 10 km altitude and for a propagation distance of 1000 km. At VLF, the waveform shapes are nearly identical to the vertical source sferics, and the amplitudes are comparable. The field amplitude at ELF is significantly lower than for a vertical source because this source orientation couples to E_x, which is weaker than E_z in the field structure for the single propagating mode at ELF.

The fields radiated from a horizontal dipole source oriented in the y direction (transverse to propagation, referred to as the "broadside" configuration) are significantly different. Such a source only excites the transverse electric (TE) wave fields, namely, E_y, B_x, and B_z [*Pappert and Ferguson*, 1986]. Figure 6 shows shows E_y, cB_x, and cB_z waveforms and spectra for a broadside horizontal source at 10 km altitude and for a propagation distance of 1000 km. Compared to sferics from a vertical or end-fire source, these waveforms have more energy below 10 kHz which is a consequence of the characteristics of the TE modes launched by this source orientation. A significant difference between TE and TM modes in a lossy parallel-plate waveguide is that TE modes are, in general, less attenuated than TM modes [*Ramo et al.*, 1984, p. 407], and this is also known to be true in the terrestrial Earth-ionosphere waveguide [*Sukhorukov*, 1996]. This leads to less attenuation and therefore higher signal amplitudes for $f < 10$ kHz. Essentially, no ELF energy is radiated for the horizontal broadside orientation because the field structure for the the single propagating mode at ELF does not contain any of the TE field components. Thus the ELF mode cannot be excited by this source orientation.

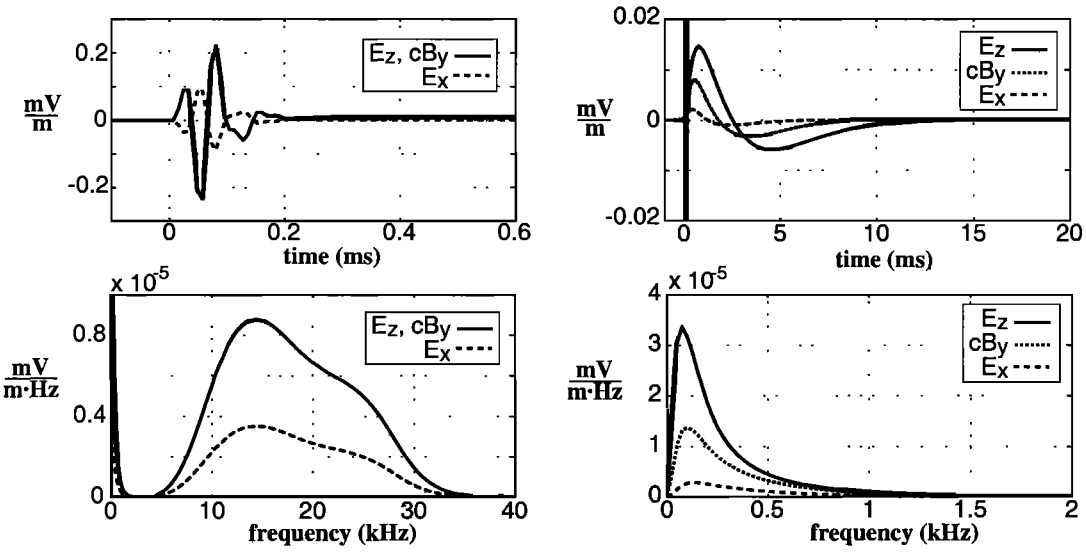

Figure 5. E_z, cB_y, and E_x sferic waveforms and spectra observed at a propagation distance of 1000 km under a daytime Martian ionosphere. The source current is in a horizontal end-fire configuration at 10 km altitude.

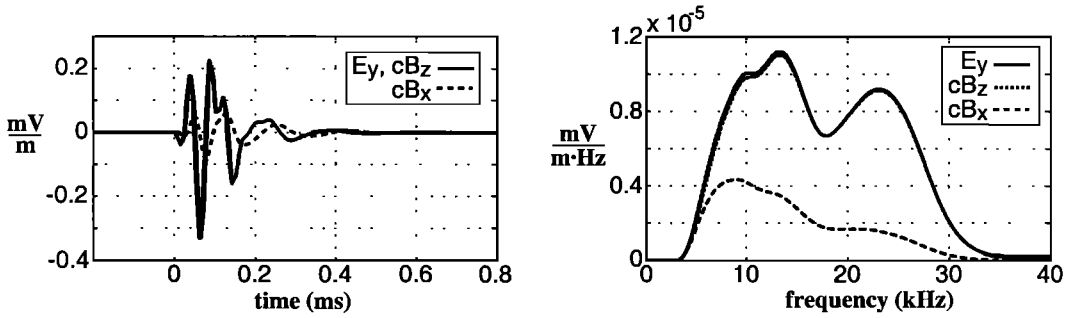

Figure 6. E_y, cB_z, and cB_x sferic waveforms and spectra observed at a propagation distance of 1000 km under a daytime Martian ionosphere. The source current is in a horizontal broadside configuration at 10 km altitude.

3.3. Differences Between Terrestrial and Martian Sferics

The calculated Martian sferics show some significant differences from terrestrial sferics. First, for the assumed Martian ionospheres, Martian sferics display a lack of diurnal variation, while there are significant differences between nighttime and daytime terrestrial sferics [*Chapman and Pierce*, 1957] due to the substantial changes between the daytime and nighttime ionospheric D region. On Earth, VLF attenuation rates at night can be less than a few decibels per 1000 km [*Wait and Spies*, 1965], leading to highly dispersed sferics with tails lasting tens of milliseconds [e.g., *Cummer et al.*, 1998]. With the ionospheric electron density profiles assumed herein, the modeled Martian sferics are similar to daytime terrestrial sferics [*Chapman and Pierce*, 1957] and contain very little dispersion because of the higher attenuation rates. However, expected Martian VLF and ELF attenuation rates are even higher than for terrestrial daytime because of the poorly conducting (and therefore poorly reflecting) ground.

Another significant difference between terrestrial and Martian sferics is in the horizontal electric field and vertical magnetic field components. On Earth, the ground conductivity is sufficiently high that the ground is a good conductor at VLF and ELF. Enforcement of the electromagnetic boundary conditions requires that the tangential electric field and normal magnetic fields are zero at the surface of a perfect conductor [*Ramo et al.*, 1984, p. 146]; hence E_x, E_y, and B_z are not observable on the ground. We have assumed a ground conductivity which makes the Martian surface a poor conductor at VLF and ELF; hence these field components can be observed on the ground, as shown in Figures 4–6.

Also, because of the assumed negligible intrinsic magnetic field over most of Mars, the fields in the ground-ionosphere waveguide can be divided into completely independent TE and TM modes. On Earth, the ambient magnetic field creates anisotropy in the upper boundary of the waveguide (i.e., the ionosphere), which mixes the TE and TM modes. This leads to mode fields which can only be classified as quasi-transverse magnetic (QTM) and quasi-transverse electric (QTE), depending on the dominant polarization of the mode. Therefore, on Mars, a vertical source current only excites higher-loss TM modes, while on Earth a vertical source excites both QTM and lower-loss QTE modes.

4. Possible Remote Sensing Applications

The above calculations of ELF-VLF propagation characteristics on Mars depend on our assumptions of the ionospheric and ground parameters. Should sferics ever be observed on Mars, a comparison of expected and actual characteristics could yield significant information about both.

The simulated Martian sferics have two main characteristics controlled at least in part by the assumed lower ionosphere: the lack of dispersion in the waveforms and the lack of a significant difference between daytime and nighttime sferics. If Martian sferics were found to be strongly dispersed like their terrestrial counterparts, this could imply a better reflecting ionosphere than we have assumed here, which, in turn, would imply a larger electron density altitude gradient. Similarly, a significant difference between daytime and nighttime Martian sferics would imply a larger diurnal ionospheric variability than that assumed here. These ionospheric characteristics could also be quantified with a technique similar to that used by *Cummer et al.* [1998] with terrestrial sferics.

The conductivity of the ground also controls many observable characteristics of sferics, including the amount of dispersion, the presence or absence of horizontal electric and vertical magnetic fields on the surface, and perhaps most strongly the amplitude of the sferic for a source of fixed strength. If the propagation distance of individual sferics can be estimated, either from multi-point measurements, from an analysis of the dispersion characteristics of individual waveforms [e.g., *Grandt*, 1992], or from orbital imaging of the source dust storm, then a statistical analysis of sferic

amplitude as a function of distance (such as would be provided by a moving storm) would yield information about the large-scale ground conductivity. We divide the following analysis of such a technique into two frequency ranges: VLF, taken to be $f > 2$ kHz, and ELF, taken to be $f < 2$ kHz.

Figure 7a shows the peak VLF E_z sferic waveform amplitude as a function of distance over a range of ground conductivities which span poorly conducting to nearly perfectly conducting at VLF. As above, the source is a 1 km vertical current channel with current described by (2). The attenuation with distance is a combination of energy spreading over the spherical planet and mode attenuation from waveguide losses. Figure 7a shows that the overall VLF attenuation with distance is a strong function of ground conductivity, and measurements of the slope of this amplitude curve could provide estimates of large-scale ground conductivity. A calculation of the attenuation rate for $\epsilon_{rg} = 15$ and $\sigma_g = 10^{-6}$ shown in Figure 7a indicates that ground permittivity does play a role in VLF attenuation; however, the slope of the sferic amplitude with distance curves is almost independent of ground permittivity, verifying the primary significance of ground conductivity in controlling the VLF attenuation rate.

A curious result is that the attenuation is strongest for $\sigma_g = 10^{-5}$ and decreases slightly with decreasing conductivity. This effect has been noted in previous studies of VLF attenuation rates [*Wait and Spies*, 1965] and is attributed to an effect similar to the Brewster angle effect [*Ramo et al.*, 1984, p. 309], in which there are particular ground parameters and wave incidence angles that produce a minimum in the reflected energy. These results show that if the attenuation rate with distance of Martian sferics could be measured, the bulk ground conductivity could be estimated within the range of σ_g=10^{-6}–10^{-2} mho m^{-1}.

Figure 7b shows in a similar manner the peak ELF E_z sferic waveform amplitude versus distance for the same range of ground conductivities. The amplitude attenuation with distance is smaller for ELF than for VLF, and, at some distance which depends on the ground conductivity, the ELF portion of the sferic becomes larger than the VLF portion. As was found for the VLF sferic amplitude, the ELF attenuation with distance curves show a clear dependence on ground conductivity. The ELF attenuation is sensitive to smaller ground conductivities, and these ELF measurements could resolve ground conductivities lower than $\sim 10^{-5}$ mho m^{-1}.

A calculation of the ground reflection coefficient at VLF and ELF for normal incidence shows why the different sensitivities to ground conductivity of the different frequency ranges is expected. Although the actual waveguide fields are effectively at oblique incidence to the ground, an analysis at normal incidence gives good physical insight and reasonably accurate quantitative results. In a lossy dielectric, the index of refraction n_g is given by

$$n_g = \left(\epsilon_{rg} - \frac{i\sigma_g}{\epsilon_0 \omega}\right)^{1/2}, \tag{3}$$

where ϵ_{rg} is the relative permittivity of the ground, σ_g is the ground conductivity, ϵ_0 is the absolute permittivity of free space, and ω is the radian wave frequency. The reflection coefficient of a plane wave normally incident on the ground from free space is then given by

$$R = \frac{n_g^{-1} - 1}{n_g^{-1} + 1}. \tag{4}$$

For $\omega = 2\pi \times 10^4$ rad s^{-1} (representative of VLF) and $\epsilon_{rg} = 5$, the magnitude of the reflection coefficient is $\sim$0.38 for $\sigma_g < 10^{-6}$ mho m^{-1}, and rises steadily to unity with increasing σ_g, reaching a value of 0.99 at $\sigma_g = 10^{-2}$ mho m^{-1}. Because the guided wave attenuation rate is in part proportional to the leakage of the energy into the ground (which, in turn, is inversely proportional to the magnitude of the ground reflection coefficient), the attenuation rate only varies significantly

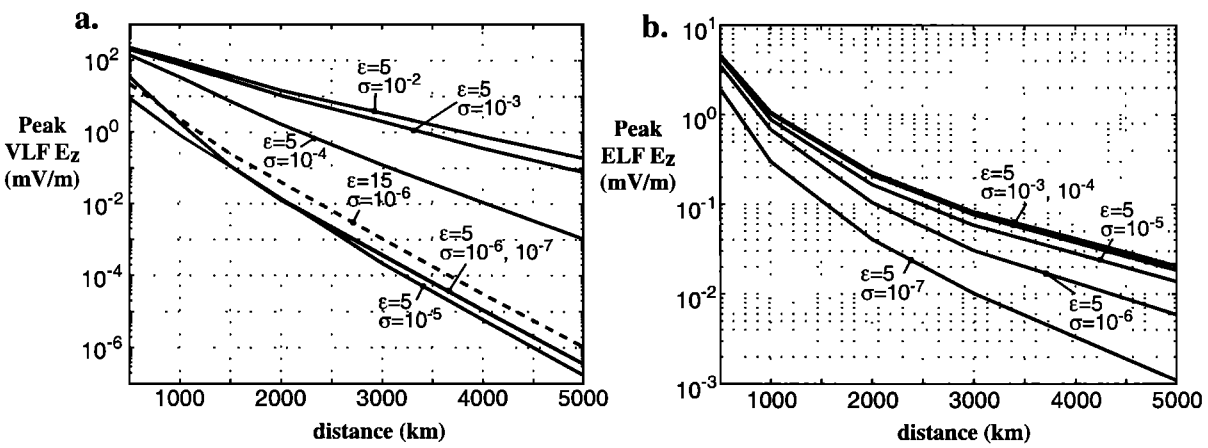

Figure 7. Variation of peak (a) VLF and (b) ELF E_z with propagation distance for a vertical discharge. The attenuation rate depends strongly on ground conductivity but over different ranges of conductivity for the two frequency ranges.

with ground conductivity in this range of σ_g. This is precisely what the full numerical calculations in Figure 7a show, and the 4 decade range of significant σ_g agrees quite well with the rough calculations above.

If the wave frequency is reduced to $\omega = 2\pi \times 10^2$ rad s^{-1} (representative of ELF), the values of σ_g for which the normal incidence ground reflection coefficient (and therefore the attenuation rate) varies significantly are reduced by a factor of 100. This agrees with the numerical results in Figure 7b which show a saturation of the ELF attenuation rate at $\sigma_g \approx 10^{-4}$ mho m^{-1}, compared to a saturation of the VLF attenuation rate at $\sigma_g \approx 10^{-2}$ mho m^{-1}.

5. Conclusions

Postulating the existence of VLF- and ELF-radiating electrical discharges associated with dust storms on Mars (see *Farrell et al.* [1999] for a thorough discussion of this possibility), we have calculated radio atmospheric waveforms and spectra for expected characteristics of the Martian ground and ionosphere. The calculations were made using a numerical model which accounts for arbitrary homogeneous ground parameters and ionospheric electron density and collision frequency altitude profiles. Assuming a source current similar to terrestrial cloud-to-ground lightning, we calculated waveforms and spectra for a variety of discharge orientations and a variety of observed field components. Because the radiation and propagation of this energy is linear, the results in this work can be considered generic and can be modified to account for stronger, weaker, or slower source discharges

A number of characteristics of the modeled Martian sferics are significantly different from those of their terrestrial counterparts. Martian sferics are expected to be similar for propagation under both daytime and nighttime Martian ionospheres, while terrestrial sferics are known to change drastically from day to night. The modeled Martian sferics are similar to daytime terrestrial sferics in that they are not strongly dispersed, which is due to the relatively small gradient of the index of refraction in the assumed Martian ionosphere and the assumed poorly conducting Martian ground. The poorly conducting Martian ground also allows nonzero tangential electric and normal magnetic fields to be observed on the Martian surface, while on Earth the almost perfectly conducting ground (at VLF and ELF) forces these components to be zero at ground level.

We also investigated the possibility of remotely sensing ionospheric and ground parameters from Martian sferics. If Martian sferics showed a strong diurnal variation or were more strongly dispersed than those presented in this paper, that would imply different ionospheric characteristics than those assumed here. The attenuation rate of sferics with distance was shown to depend strongly on the ground conductivity. If this quantity could be measured either with multilocation measurements or dispersion analyses of individual waveforms, the large-scale Martian ground conductivity could be estimated thereby providing a unique method to probe for large-scale subsurface conductivity features, such as regions containing high-conductivity minerals, ice, or water.

References

Anderson, R., S. Björnsson, D. C. Blanchard, S. Gathman, J. Hughes, S. Jónasson, C. Moore, H. Survilas, and B. Vonnegut, Electricity in volcanic clouds, *Science, 148*, 1179, 1965.

Banks, P. M., and G. Kockarts, *Aeronomy (Part A)*, Academic, San Diego, Calif., 1973.

Bilitza, D., International Reference Ionosphere—Status 1995/1996 *Adv. Space Res., 20(9)*, 1751, 1997.

Budden, K. G., *The Wave-Guide Mode Theory of Wave Propagation*, Logos, London, 1961.

Budden, K. G., *The Propagation of Radio Waves*, Cambridge Univ. Press, New York, 1985.

Chapman, J., and E. T. Pierce, Relations between the character of atmospherics and their place of origin, *Proc. IRE, 45*, 804, 1957.

Crozier, W. D., The electric field of a New Mexico dust devil, *J. Geophys. Res., 69*, 5427, 1964.

Cummer, S. A., U. S. Inan, and T. F. Bell, Ionospheric D region remote sensing using VLF radio atmospherics, *Radio Sci., 33*, 1781, 1998.

Eden, H. F., and B. Vonnegut, Electrical breakdown caused by dust motion in low-pressure atmospheres: Considerations for Mars, *Science, 180*, 962, 1973.

Farrell, W. F., M. L. Kaiser, M. D. Desch, J. G. Houser, S. A. Cummer, D. M. Wilt, and G. A. Landis, Detecting electrical activity from Martian dust storms, *J. Geophys. Res., 104*, 3795, 1999.

Goldman, M., and F. M. Neubauer, Groundwater exploration using integrated geophysical techniques, *Surv. Geophys., 15*, 331, 1994.

Grandt, C., Thunderstorm monitoring in South Africa and Europe by means of very low frequency sferics, *J. Geophys. Res., 97*, 18215, 1992.

Greifinger, C., and P. Greifinger, Noniterative procedure for calculating ELF mode constants in the anisotropic earth-ionosphere waveguide, *Rad. Sci, 21*, 981, 1986.

Hake, R. D., and A. V. Phelps, Momentum-transfer and inelastic-collision cross sections for electrons in O_2, CO, and CO_2, *Phys. Rev., 158*, 70, 1967.

Hanson, W. B., S. Sanatani, and D. R. Zuccaro, The Martian ionosphere as observed by the Viking retarding potential analyzers, *J. Geophys. Res., 82*, 4351, 1977.

Jones, D. L., Electromagnetic radiation from multiple return strokes of lightning, *J. Atmos. Terr. Phys., 32*, 1077, 1970.

MacElroy, M. B., T. Y. Kong, and V. L. Yung, Photochemistry and evolution of Mars' atmosphere: A Viking perspective, *J. Geophys. Res., 82*, 4379, 1977.

Olhoeft, G. R., Ground penetrating radar on Mars, *Proc. of Seventh Intl. Conf. on Ground Penetrating Radar*, 387, 1998.

Olhoeft, G. R., and D. W. Strangway, Electrical properties of the surface layers of Mars, *Geophys. Res. Lett., 1*, 141, 1974.

Oppenheim, A. V., and R. W. Schafer, *Discrete-Time Signal Processing*, Prentice-Hall, Englewood Cliffs, N. J., 1989.

Pappert, R. A., and J. A. Ferguson, VLF/LF mode conversion model calculations for air to air transmissions in the Earth-ionosphere waveguide, *Radio Sci., 21*, 551, 1986.

Ramo, S., J. R. Whinnery, and T. Van Duzer, *Fields and Waves in Communication Electronics*, New York, New York: John Wiley, 1984.

Sentman, D. D., Detection of elliptical polarization and mode splitting in discrete Schumann resonance excitations, *J. Atmos. Terr. Phys., 51*, 507, 1989.

Sukhorukov, A. I., On the Schumann resonances on Mars, *Planet. Space Sci., 39*, 1673, 1991.

Sukhorukov, A. I., ELF-VLF atmospheric waveforms under night-time ionospheric conditions, *Ann. Geophys., 14*, 33, 1996.

Tyler, G. L., D. B. Campbell, G. S. Downs, R. R. Green, and H. J. Moore, Radar characteristics of Viking 1 landing sites, *Science, 193*, 812, 1976.

Wait, J. R., and K. P. Spies, Influence of finite ground conductivity on the propagation of VLF radio waves, *J. Nat. Bur. of Stand., 69D*, 1359, 1965.

Whitten, R. C., I. G. Poppoff, and J. S. Sims, The ionosphere of Mars below 80 km altitude I—Quiescent conditions, *Planet. Space Sci., 19*, 243, 1971.

Zhang, M. H. G., J. G. Luhmann, and A. J. Kliore, An observational study of the nightside ionospheres of Mars and Venus with radio occultation methods, *J. Geophys. Res., 95*, 17095, 1990.

Steven A. Cummer and William M. Farrell, Laboratory for Extraterrestrial Physics, NASA Goddard Space Flight Center, Greenbelt, MD 20771. (steve.cummer@gsfc.nasa.gov; farrell@faltraz.gsfc.nasa.gov)

(Received September 22, 1998; revised March 15, 1999; accepted March 25, 1999.)